| Journal of Coastal Research | SI 64 | 2042 - 2047 | ICS2011 (Proceedings) | Poland | ISSN 0749-0208 |
|---|---|---|---|---|---|

# Mapping the internal wave field in the Baltic Sea in the context of sediment transport in shallow water

**O. Kurkina†‡∞, T. Talipova§, E. Pelinovsky‡∞§ and T. Soomere†**

† Institute of Cybernetics at Tallinn University of Technology, Tallinn, EE-12618, Estonia, soomere@cs.ioc.ee

‡ State University, Higher School of Economics, Nizhny Novgorod Branch, Nizhny Novgorod, Russia, Oksana.Kurkina@mail.ru

∞ Nizhny Novgorod State Technical University, Nizhny Novgorod, Russia pelinovsky@hydro.appl.sci-nnov.ru

§ Institute of Applied Physics of Russian Academy of Sciences, Nizhny Novgorod, Russia tgtalipova@mail.ru

**ABSTRACT**

Kurkina, O.; Pelinovsky, E.; Talipova, T., and Soomere, T., 2011. Mapping the internal wave field in the Baltic Sea in the context of sediment transport in shallow water. Journal of Coastal Research, SI 64 (Proceedings of the 11th International Coastal Symposium), 2042 – 2047. Szczecin, Poland, ISSN 0749-0208

The geographical and seasonal distributions of kinematic and nonlinear parameters of long internal waves obtained on a base of GDEM climatology in the Baltic Sea region are examined. The considered parameters (phase speed of long internal wave, dispersion, quadratic and cubic nonlinearity parameters) of the weakly-nonlinear Korteweg-de Vries-type models (in particular, Gardner model), can be used for evaluations of the possible polarities, shapes of solitary internal waves, their limiting amplitudes and propagation speeds. The key outcome is an express estimate of the expected internal wave parameters for different regions of the Baltic Sea. The central kinematic characteristic is the near-bottom velocity in internal waves in areas where the density jump layers are located in the vicinity of seabed. In such areas internal waves are the major driver of sediment resuspension and erosion processes and may be also responsible for destroying the laminated structure of sedimentation regime (that frequently occurs in certain areas of the Baltic Sea).

**ADDITIONAL INDEX WORDS:** *density stratification, internal soliton, Korteweg-de Vries equation, Gardner equation*

## INTRODUCTION

Large-amplitude internal waves (IW) are often very energetic events in stratified and coastal marine environments. They have a significant role in particle transport and mixing of water masses, as well as affecting acoustic propagation. Understanding the impact of large IW is of key importance in the coastal marine environment. The regional aspect is essential in IW studies as the vertical stratification of the ocean is highly inhomogeneous in the horizontal direction. Here the attention is drawn t the Baltic Sea which is strongly influenced by wind forcing and buoyancy, that causes mesoscale variability of hydrological fields with horizontal scales of 5–20 km. The Baltic Sea is known as non tidal region and generation of IW is mainly accounts for the strong winds. The cyclones propagating with the winds of 10–15 m/s here cause the generation of IW with amplitudes of 11–15 m, while the current velocities in the upper layer are about 11–15 cm/s, and in the lower layer, they are about 5–8 cm/s (Chernysheva, 1987). The characteristics of IW measured in the Baltic Sea are given in (Kol'chitskii *et al.*, 1996; Golenko and Mel'nikov, 2007). In particular, IW with periods of 0.1–1 h, observed in the central part of the Gotland Deep, formed internal wave trains with duration of several hours and current amplitudes of about 3 cm/s. IW in the inertial frequency range can induce wave currents with velocities reaching 20 cm/s.

The horizontal variability of hydrological fields becomes evident in the weakly nonlinear internal wave theory (Talipova et al., 1998; Holloway et al, 1999; Pelinovsky et al, 2007) as spatial variability of the coefficients of the corresponding nonlinear evolution equations. These coefficients, such as propagation speed, quadratic and cubic nonlinearities and dispersion, represent the kinematic characteristics of internal wave field. Horizontal variability of vertical stratification is especially evident in the sea shelf zones and shallow-water basins of estuary type.

When IW are modeled numerically, an important problem is to specify the hydrological conditions determining density variations with depth to initialize the numerical models. An adequate way is to use gridded temperature-salinity data from international hydrological atlases. This approach allows reproducing the internal "weather" of the considered basin, because hydrological atlases represent the long-term mean density stratifications.

The aim of this study is to examine the geographical and seasonal distributions of kinematic parameters of long IW obtained on a base of GDEM (Generalized Digital Environmental Model) climatology in the Baltic Sea region. This data set reflects the global climatology of the temperature and salinity of the global oceans.

The first such estimations for the Baltic Sea are given in (Talipova et al., 1998) for the region of the Gotland Basin. The considered kinematic parameters can be used for express-evaluations of the possible polarities, shapes of solitary IW, their limiting amplitudes, propagation speeds, etc. They also can help to set-up and initialize more complex models for internal gravity waves (IGW, MIT GCM, POM).

We present overview of spatial variability of the listed parameters and several interesting features of the underlying hydrophysical fields such as the depth of the maximal value in the Brunt-Vaisala frequency (BVF) profile and the maximal values of the BVF over such profiles for different months. The averaged values of coefficients of the Gardner equation allow producing the estimations of nonlinear IW shapes and limiting amplitudes before numerical simulations.

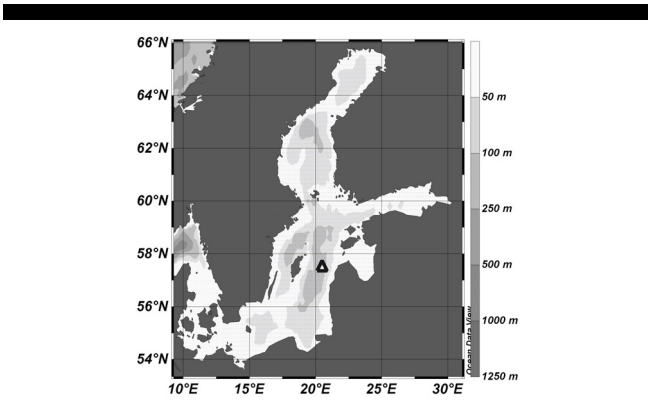


Figure 1. Bathymetry of the Baltic Sea. The triangle shows the location of measurements presented in Fig. 12.

The key outcome of our calculations is an express estimate of the expected internal wave parameters for different regions of the

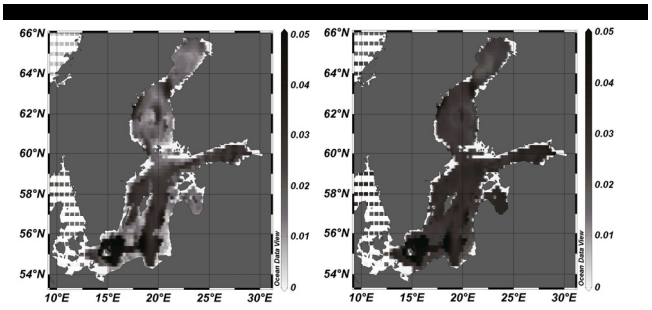


Figure 2. Maximal value in the BVF profile [$s^{-1}$] (left panel: January, right panel: July).

Baltic Sea. The central IW field characteristic is the near-bottom velocity in IW in areas where the density jump layers are located in the vicinity of seabed. In such areas IW are the major driver of sediment resuspension and erosion processes and may be also responsible for destroying the laminated structure of sedimentation regime (that frequently occurs in certain areas of

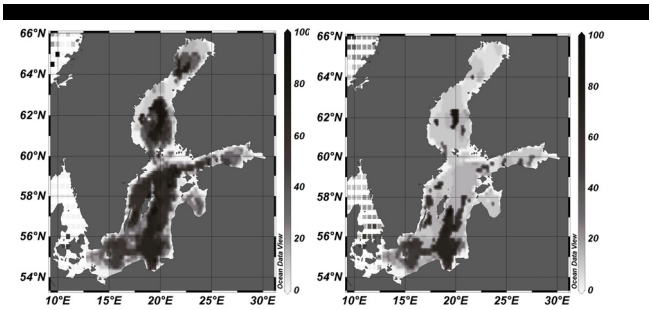


Figure 3. Depth [m] of maximal value in the Brunt-Vaisala frequency profile (left panel: January, right panel: July).

the Baltic Sea). As the pycnocline is in many cases located at a depth of only a few meters in some areas of the Baltic Sea during spring and summer (Leppäranta and Myrberg, 2009), the impact of IW on sedimentation processes frequently extends to the coastal

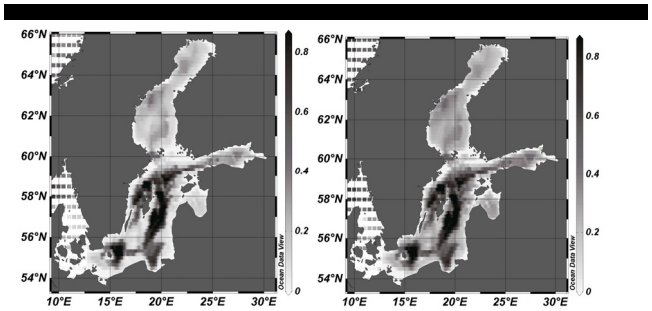


Figure 4. Long linear IW speed [m $s^{-1}$] (left panel: January, right panel: July).

zone and overlaps with the nearshore affected by surface waves. Such situation often happens in partially sheltered sub-basins of the Baltic Sea (Figure 1) such as the Gulf of Finland where the role of high near-bottom velocities, eventually created by high-amplitude IW, has been systematically underestimated in engineering applications (Erm *et al*., 2010).

## INTERNAL WAVES IN STRATIFIED BASINS

The weakly nonlinear theory of long IW in a vertical section of stratified basin assumes, that the internal wave field (in particular, the vertical isopycnal displacement $\zeta(z,x,t)$ ) can be expressed as a series (up to the 2nd in nonlinearity) (Pelinovsky *et al*., 2007):

$$\zeta(z,x,t) = \eta(x,t)\Phi(z) + \eta^2(x,t)F(z) \qquad (1)$$

where $x$ is horizontal axis, $z$ is vertical axis directed upward, $t$ is time, $\eta(x,t)$ describes the transformation of a wave along the axis of propagation and its evolution in time. Function $\Phi(z)$ (the vertical mode) describes vertical structure of long internal wave, and $F(z)$ is the first nonlinear correction to $\Phi(z)$. $\Phi(z)$ is a solution of an eigenvalue problem, which can be written in the form (in Boussinesq approximation usually valid for natural sea stratifications):

$$\frac{d^2\Phi}{dz^2} + \frac{N^2(z)}{c^2}\Phi = 0, \quad \Phi(0) = \Phi(H) = 0 \qquad (2)$$

here eigenvalue $c$ is the phase speed of long linear internal wave, $H$ is the total water depth, $N(z)$ is the Brunt-Väisälä frequency (BVF) determined by the expression:

$$N^2(z) = -\frac{g}{\rho(z)}\frac{d\rho(z)}{dz}, \qquad (3)$$

$g$ is gravity acceleration and $\rho(z)$ is undisturbed density profile. It is well known, that problem (2) has an infinite number of eigenvalues $c_1>c_2>c_3>\ldots$ and corresponding eigenfunctions $\Phi_1$, $\Phi_2$, $\Phi_3$,… We consider only the first (lowest) mode, when the function $\Phi$ has a single zero at $z=0$ and $z=H$. This mode is usually the most energetic in the internal wave spectrum. It is convenient to normalize the solution so that the maximum of $\Phi(z)$ is $\Phi_{\max} = \Phi(z_{\max}) = 1$.

In this case the leading order solution $\eta(x, t)$ coincides with the isopycnal surface displacement at $z_{\max}$:

$$\zeta(x, z_{\max}, t) = \eta(x,t) \qquad (4)$$

Function $F(z)$ can be found as a solution of the inhomogeneous boundary problem:

$$\frac{d^2F}{dz^2} + \frac{N^2}{c^2}F = -\frac{\alpha}{c}\frac{d^2\Phi}{dz^2} + \frac{3}{2}\frac{d}{dy}\left[\left(\frac{d\Phi}{dz}\right)^2\right], \qquad (5)$$

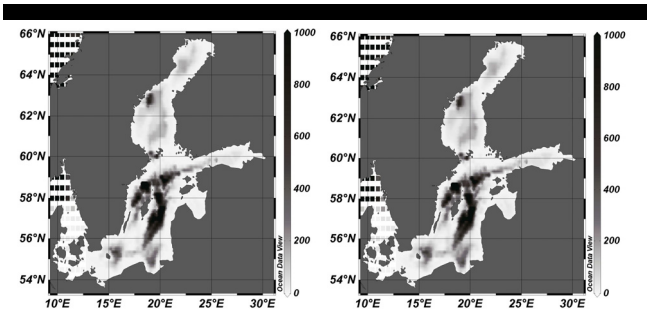


Figure 5. Long linear IW dispersion parameter [$m^3 \cdot s^{-1}$] (left panel: January, right panel: July).

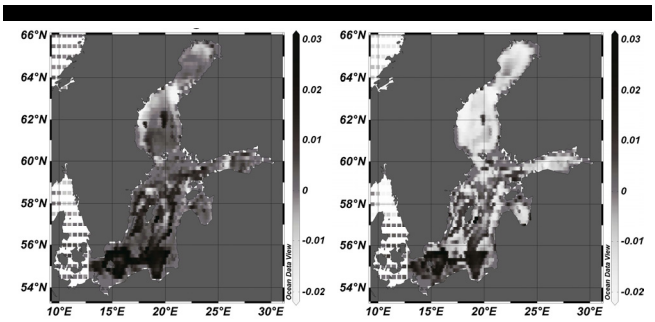


Figure 6. Quadratic nonlinearity parameter [$s^{-1}$] (left panel: January, right panel: July).

$$F(0) = F(H) = 0\,,$$

where the auxiliary normalization condition $F(z_{max})=0$ is used to determine the solution uniquely.

In this model, the function $\eta(x,t)$ satisfies the nonlinear evolution equation (extended Korteweg-de Vries (KdV) or Gardner equation):

$$\frac{\partial \eta}{\partial t} + \left(c + \alpha\eta + \alpha_1\eta^2\right)\frac{\partial \eta}{\partial x} + \beta\frac{\partial^3 \eta}{\partial x^3} = 0\,. \qquad (6)$$

This equation contains cubic nonlinearity, the presence of which provides better predictions of wave form, especially in the coastal zone. The coefficients of this equation are determined through the $\Phi(z)$ and $F(z)$:

$$\beta = \frac{c}{2D}\int_0^H \Phi^2 dz\,,\ \alpha = \frac{3c}{2D}\int_0^H \left(\frac{d\Phi}{dz}\right)^3 dz\,,\ D = \int_0^H \left(\frac{d\Phi}{dz}\right)^2 dz \qquad (7)$$

$$\alpha_1 = \frac{1}{2D}\int_0^H dz\left\{9c\frac{dF}{dz}\left(\frac{d\Phi}{dz}\right)^2 - 6c\left(\frac{d\Phi}{dz}\right)^4 + 5\alpha\left(\frac{d\Phi}{dz}\right)^3 - \right.$$
$$\left. - 4\alpha\frac{dF}{dz}\frac{d\Phi}{dz} - \frac{\alpha^2}{c}\left(\frac{d\Phi}{dz}\right)^2\right\} \qquad (8)$$

In the present paper we construct and discuss the geographical charts for parameters $c$, $\beta$, $\alpha$ and $\alpha_1$ of the Gardner equation (6) in the Baltic Sea region, using climatological oceanographic data and calculating Brunt-Väisälä frequency (3) from temperature and salinity profiles.

## KINEMATIC CHARACTERISTICS OF THE INTERNAL WAVE FIELD IN THE BALTIC SEA

We use long-term mean temperature and salinity profiles from GDEM-V3.0 (Teague et al., 1990) to calculate density stratifications for the Baltic Sea. With these profiles speed of propagation, dispersive and both nonlinear parameters of the Gardner equation are computed and presented in the form of charts with a resolution of 10'×10' along latitudes and longitude. We also discuss spatial and seasonal (July and January) variations of these parameters. GDEMs at 10 minute resolution have been developed for selected regions where data is sufficient to support the higher resolution; particularly, such data are available for the Baltic Sea.

Visualization of results was done using the software Ocean Data View (Schlitzer, 2010).

The bathymetry of the Baltic Sea (Figure 1) and charts representing the magnitude of seasonal variability of the density stratification (in terms of maxima of BVF (Figure 2) and the depth where the maximum of BVF occurs (Figure 3)) can help in the interpretation of obtained results and in explaining the features of the geographical distribution of kinematic parameters of the IW field. Figures 2 and 3 demonstrate that stratification data strongly depend on the particular season. Note the increase in the maximal BVF values during summer simultaneously with a decrease of their depths. So, in general one can expect an increase in the impact of IW upon the sediment transport in shallow-water regions of the Baltic Sea in late summer and autumn.

Seasonal variations in the linear parameters $c$, $\beta$ (Figures 4 and 5) are not very significant. Also the main features of their geographical distribution do not change from season to season. The maximal value of $c$ is about 90 cm/s. These parameters apparently are mostly determined by the bathymetry. However the nonlinear parameters $\alpha$, $\alpha_1$ (Figures 6 and 7) are more sensitive to the fine structure of the density stratification. Their seasonal variability is significant, and they can even change their signs from season to season. The quadratic nonlinearity parameter changes from –0.02 to 0.03 $s^{-1}$ and for July (Figure 6, right panel) it is mainly positive in the southern part of the Baltic Sea (the Arcona Basin, the Bornholm Basin and the Slupsk Furrow), in the central part (the Gotland Basin) there are the spots of different signs of $\alpha$, and the Gulf of Finland and the Bothnian Sea are characterized by the negative value of this parameter. In winter season (Figure 6, left panel) the zone of positive values broadens including the central part of the Baltic Sea and most of the Gulf of Finland. The cubic nonlinear parameter (Figure 7), which changes from –0.003 to 0.004 $m^{-1}s^{-1}$, shows the spotty character of the zones with positive and negative values with the predominance of negative values in winter (Figure 7, left panel) the positive values in the Bothnian Sea in summer (Figure 7, right panel).

## SHAPES OF NONLINEAR INTERNAL WAVES

Let us consider the single-soliton solution of Eq. (6):

$$\eta(x,t) = \frac{A}{1 + B\mathrm{ch}(\gamma(x - Vt)),} \qquad (9)$$

where the soliton velocity $V = c + \beta\gamma^2$ is expressed through the inverse width of soliton, $\gamma$, and the soliton amplitude, $a$, or the extremum of the function (9), is

$$a = \frac{A}{1+B}\,,\ \text{and}\quad A = \frac{6\beta\gamma^2}{\alpha},\qquad B^2 = 1 + \frac{6\alpha_1\beta\gamma^2}{\alpha^2}\,. \qquad (10)$$

Let us consider in detail now the possible combinations of the signs of the nonlinear coefficients in the Gardner equation.

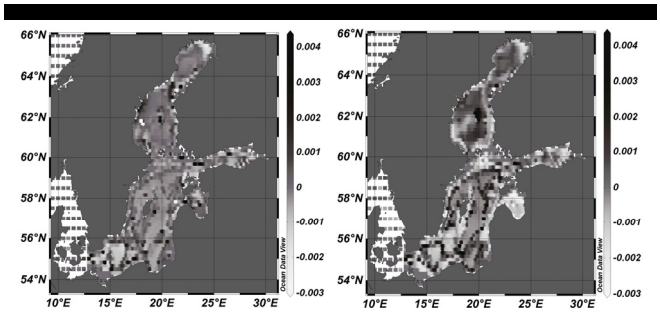

Figure 7. Cubic nonlinearity parameter [$m^{-1} \cdot s^{-1}$] (left panel: January, right panel: July).

## Korteweg-de Vries soliton

When the cubic nonlinearity vanishes ($\alpha_1 = 0$), the solution (9) is reduced to the classical Korteweg-de Vries (KdV) soliton:

$$\eta(x,t) = a\,\mathrm{sech}^2\left[\sqrt{\frac{\alpha a}{12\beta}}\left(x - \left[c + \frac{\alpha a}{3}\right]t\right)\right]. \qquad (11)$$

It has only one polarity defined by the sign of quadratic nonlinearity $\alpha$.

## Gardner soliton

When the cubic nonlinear coefficient $\alpha_1$ is negative, soliton

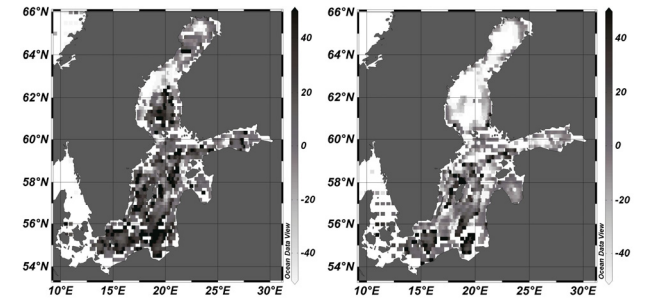

Figure 8. Limiting amplitudes [m] of "top-table" solitary waves (for negative cubic nonlinearity values, left panel: January, right panel: July).

solutions of single polarity, with $\alpha\eta > 0$, exist with amplitudes between zero and a limiting value

$$a_{\lim} = \frac{\alpha}{|\alpha_1|}. \qquad (12)$$

The soliton shapes for different combinations of signs of nonlinear parameters are discussed in details in (Pelinovsky et al, 2007). The increase in the soliton amplitude to the limiting value (12) ($B \to 0$) leads to the unlimited increase of its width. The solitary wave becomes "wide", or "table-shaped." It has a flat crest, and its slopes are shock-like waves, or kinks.

If $\alpha_1 > 0$, soliton families of either polarity exist. One of these families with $\alpha\eta > 0$ has $1 < B < \infty$, and the amplitude is not bounded. For large amplitudes ($B \to \infty$) the solution has the shape of the soliton of the modified KdV equation:

$$\eta(x,t) = a\,\mathrm{sech}\left[\sqrt{\frac{\alpha_1 a^2}{6\beta}}\left(x - \left[c + \frac{\alpha_1 a^2}{6}\right]t\right)\right]. \qquad (13)$$

Another family of solitons (with $\alpha\eta < 0$) corresponds to negative $B$ ($-\infty < B < -1$). At $B \to -\infty$ such solitons are transformed into the modified KdV soliton (13). Waves of this family have a minimum amplitude $a_{\mathrm{alg}} = -2\alpha/\alpha_1$.

At near-critical amplitudes ($B \to -1$) soliton (9) tends to so-called "algebraic" soliton:

$$\eta(x) = \frac{a_{\mathrm{alg}}}{1 + \alpha^2 (x - ct)^2 / 6\beta}, \quad V = c. \qquad (14)$$

Note that its speed is equal to linear long wave speed. In the gap between the zero and $a_{\mathrm{alg}}$ there are no any solitons.

Figures 8 and 9 illustrate geographical distributions of amplitudes $a_{\lim}$ (12) for the points with negative cubic nonlinearity and $a_{\mathrm{alg}}$ (15) for the points with positive cubic nonlinearity values in the Baltic Sea. The range for the values of these amplitudes is about ±40 m.

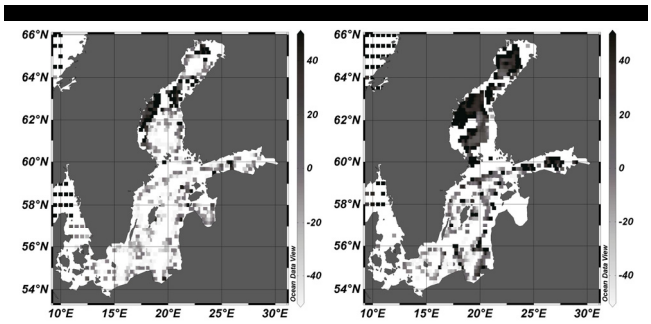

Figure 9. Amplitudes [m] of algebraic solitons (left panel: January, right panel: July).

# HORIZONTAL VELOCITY

With the use of Eq. (1) the components of velocities of fluid particles ($u$, $w$) in the vertical section ($x$, $z$) can be expressed as follows:

$$u(x,z,t) = c\,\eta(x,t)\frac{d\Phi}{dz} + \left(\frac{\alpha}{2}\frac{d\Phi}{dz} + c\frac{dF}{dz}\right)\eta^2, \qquad (15)$$

$$w(x,z,t) = -c\frac{\partial \eta}{\partial x}\Phi(z) - \left(\alpha\Phi(z) + 2cF(z)\right)\eta\frac{\partial \eta}{\partial x}, \qquad (16)$$

The horizontal velocity component $u$ gives the greatest contribution into the local current speed. This is typical for long waves and this characteristic of internal wave field must be considered in the analysis of near-bottom processes connected with sediment transport.

The first terms in Eqs. (15) and (16) correspond to the leading order of the asymptotic expansion. The remaining additives reflect the first nonlinear correction in the asymptotic series. Thus, for the forecast of the local current speed one has to determine the isopycnal displacement $\eta(x, t)$ at the level of $z_{\max}$ (see (4)), the vertical IW mode $\Phi(z)$ and its nonlinear correction $F(z)$. The amplitude of $\eta(x, t)$ is not known a priori, it depends upon a large number of background conditions of internal wave generation, and can be found by means of the detailed simulation.

For the analysis of the geographical features of the near-bottom velocity distribution it is convenient to consider a normalized quantity $u/\eta$ (Figure10). To the leading order, it is independent of

$\eta$. The largest values of near-bottom velocities can be expected along all the coasts, especially in the eastern part of the Gulf of Finland and in the south-western part of the Baltic Sea (the Arcona basin and the Bornholm Basin) with the tendency to increase in the warm season.

The contribution from second-order terms in the horizontal velocity (Eq. (19)) can be estimated for the model of a three-layer stratification – a situation that frequently occurs in the Baltic Sea. The water masses in its central part often consist of a mixed upper layer, well-defined seasonal thermocline at a depth about 20–40 m, an intermediate layer and main halocline at a depth about 80–100 m. In many cases the total depth is 120–140 m and density changes between the layers are more or less equal (Soomere, 2003). We model this sort of three-layer density profile using the formula

$$\rho = \rho_0 - \Delta_{\rho_1} \tanh \frac{z - z_1}{d_1} - \Delta_{\rho_2} \tanh \frac{z - z_2}{d_2} \qquad (17)$$

where the parameters are chosen to reproduce the profiles presented in (Soomere, 2003): $\rho_0$ = 1007 [kg/m$^3$], $\Delta_{\rho 1} = \Delta_{\rho 2}$ = 2 [kg/m$^3$], $d_1$ = 3 [m], $d_2$ = 10 [m], $z_1$ = –20 [m], $z_2$ = –80 [m], total depth is 130 m. Figure 11a presents the BVF profile and corresponding lowest vertical mode $\Phi(z)$ and the nonlinear correction $F(z)$ profiles. Such background conditions give positive signs of both nonlinear parameters ($\alpha$, $\alpha_1$), and the solitons of both polarities can exist. The isopycnal displacements and horizontal velocity contours induced by the passage of the lowest-mode solitons (9) of positive and negative polarities with approximately equal amplitudes ($a \cong$ 13.4 m) are demonstrated by Figure 11b-e (for the leading order of the Eqs. (1) and (15)) and by Figure 12 (where the nonlinear correction terms are taken into account in Eqs. (1) and (15)). These figures show quasi-three-layer structure of horizontal velocity fields with thin transition layers of thicknesses $d_1$ and $d_2$. Notice that the velocity is positive when the fluid particles move in the direction of soliton propagation (to the right), and negative in the opposite case. The fields of horizontal velocities in elevation and depression solitons are positive and negative, respectively, in the lower near-bottom layer, and have the reversed in the middle and upper layer. Near-bottom and near-surface velocities reach the greatest values whereas the velocity in the mid-layer is not significant. The influence of the nonlinear correction manifests itself firstly in the shape of the lines of zero horizontal velocity: they are curved oppositely to the soliton polarity while for the leading order wave field they are horizontal. Also the wavefield accounting for the nonlinear correction has smaller maximal absolute values of negative velocities (near-surface for the soliton of elevation, and near-bottom for the soliton of depression) and larger maximal values of positive velocities.

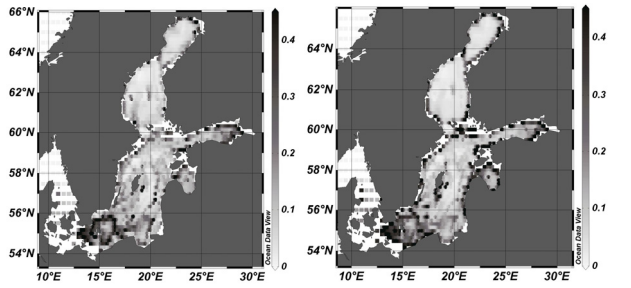


Figure 10. The value of leading-order near-bottom velocity in internal wave field divided by $\eta$ ($x$, $t$) in [1/s] (left panel: January, right panel: July).

## DISCUSSION AND CONCLUSIONS

In essence, the performed research is a step on the way towards systematic incorporation of the information about internal wave fields into engineering applications. As typical for wave processes, propagation of IW provides a mechanism of the transfer of massive quantities of energy between different sea areas. This energy is mostly released in regions where the pycnocline is located so close to the sea surface or the bottom that the large-amplitude IW will break. In the Baltic Sea conditions, this location may vary considerably and frequently occurs in areas where upper layers of soft sediments are substantially polluted (Verta *et al.*, 2007).

Water velocities in breaking IW usually largely exceed the

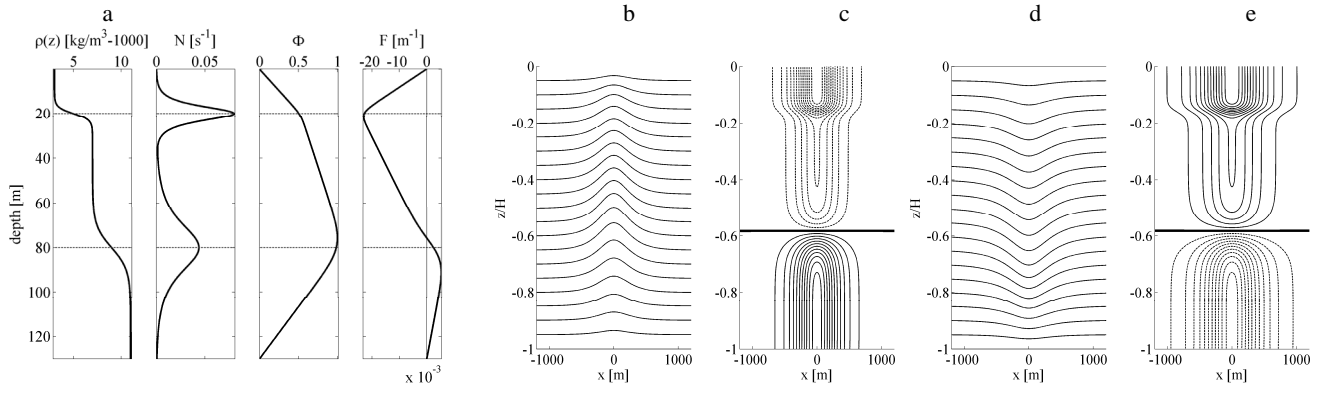


Figure 11. (a) Model of almost three-layer density stratification and corresponding profiles of Brunt-Väisälä frequency $N(z)$, lowest vertical mode $\Phi(z)$ and its nonlinear correction $F(z)$; leading order of isopycnal displacements (b, d) and horizontal velocity (c,e) contours while the soliton of positive/negative polarity propagates. In panels b, d contours are given with $H$/20 interval; in panels d, e solid/dashed lines correspond to positive/negative horizontal velocities, thick lines are the lines of zero horizontal velocity, the interval between contours is 0.025$c$.

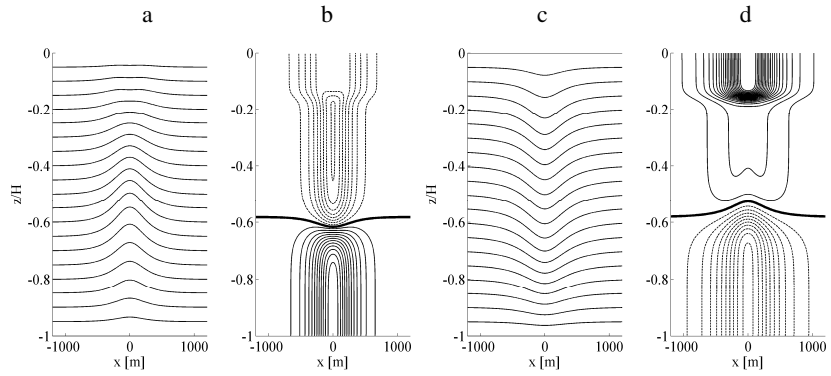


Figure 12. Isopycnal displacements (a, c) and horizontal velocity (b,d) contours while the soliton of positive/negative polarity propagates. In panels a, c contours are given with *H*/20 interval; in panels c, d solid/dashed lines correspond to positive/negative horizontal velocities, thick lines are the lines of zero horizontal velocity, the interval between contours is 0.025*c*.

threshold for suspension of such sediment. The dimensions of resulting plume are basically determined by the above-considered limiting parameters of large-scale IW. The frequently occurring process of upwelling (that has high chances to occur simultaneously with the presence of intense internal wave field) brings the pollution to the upper layers of the sea where surface currents redistribute it over a large sea area (Leppäranta and Myrberg, 2009).

The largest uncertainty of this multi-step process is currently connected with insufficient knowledge about the internal wave fields in the Baltic Sea. Therefore, in connection with detailed studies into upwelling (Lehmann and Myrberg, 2008) and current-drive transport of different adverse impacts (Soomere *et al*., 2011), our study paves the way towards much better understanding the functioning of key features of the entire Baltic Sea (eco)system and has a large potential to contribute into mitigation and management marine-induced hazards, especially problems connected with coastal pollution and coastal zone management.

## LITERATURE CITED

Erm, A.; Elken, J.; Pavelson, J.; Kask, J.; Voll, M.; Kört, M.; Roots, O.; Liblik, T.; Lagemaa, P., and Buschmann, F., 2010. Observation of high-speed deep currents and resuspension of soft sediments in the central part of the Gulf of Finland. In: *The 10th International Marine Geological Conference "The Baltic Sea Geology–10,"* 24–28 August 2010, VSEGEI, St. Petersburg, Russia. Press VSEGEI, Saint-Petersburg, pp. 25–26.

Chernysheva, E.S., 1987. On the modeling of long internal waves. In: Davidan, I.N. et al. (eds.), *Problems of the Studies and Mathematical Modeling of the Baltic Sea Ecosystem*. *Modeling of the Ecosystem Components* Issue No. 3, Leningrad, Gidrometeoizdat, pp. 50–54.

Golenko, N.N. and Mel'nikov, V.A., 2007. Estimation of spatio-temporal parameters of the internal wave field in the Southwest Baltic Sea using data by towed probe. *Scientific reports of the Russian Geographic Union (Kaliningrad branch), Russian State Univ., Kaliningrad*, Volume 5, pp. C1–C4.

Holloway, P.; Pelinovsky, E., and Talipova, T., 1999. A generalized Korteweg-de Vries model of internal tide transformation in the coastal zone. *Journal of Geophysical Research*, 104 (C8), 18333–18350.

Leppäranta, M. and Myrberg, K., 2009. *Physical oceanography of the Baltic Sea*. Springer Praxis, Berlin Heidelberg New York, 378 p.

Lehmann, A. and Myrberg, K., 2008. Upwelling in the Baltic Sea – A review. *Journal of Marine Systems*, 74 (S), S3–S12.

Kol'chitskii, N.N.; Monin, A.S., and Paka, V.T., 1996. On internal seiches in the deep Baltic Sea. *Doklady Akademii Nauk*, 346 (2), 249–255.

Pelinovsky, E.; Polukhina, O.; Slunyaev, A., and Talipova, T., 2007. Internal solitary waves. *In* Grimshaw, R. (ed.), *Solitary Waves in Fluids*. WIT Press, Southampton, Boston, pp. 85–110.

Schlitzer, R., 2010. Ocean Data View, http://odv.awi.de.

Soomere, T., 2003. Coupling coefficients and kinetic equation for Rossby waves. *Nonlinear Processes in Geophysics*, 10, 385–396.

Soomere, T.; Delpeche, N.; Viikmäe, B.; Quak, E.; Meier, H.E.M., and Döös, K., 2011. Patterns of current-induced transport in the surface layer of the Gulf of Finland. *Boreal Environment Research*, 16 (1), 1–21.

Talipova, T.; Pelinovsky, E., and Kõuts, T., 1998. Kinematics characteristics of the internal wave field in the Gotland Deep. *Oceanology*, 38 (1), 37–46.

Teague, W.J.; Carron, M.J., and Hogan, P.J., 1990. A comparison between the Generalized Digital Environmental Model and Levitus climatologies. *Journal of Geophysical Research*, 95, 7167–7183.

Verta, M.; Salo, S.; Korhonen, M.; Assmuth, T.; Kiviranta, H.; Koistinen, J.; Ruokojärvi, P.; Isosaari, P.; Bergqvist, P.-A.; Tysklind, M.; Cato, I.; Vikelsøe, J., and Larsen, M.M., 2007, Dioxin concentrations in sediments of the Baltic Sea – A survey of existing data. *Chemosphere*, 67, 1762–1775.

## ACKNOWLEDGEMENT

The research is partially supported by Russian Foundations for Basic Research grants (10-05-00199 and 09-05-00204), Estonian Science Foundation Grants (7413 and 8870), and the targeted financing by the Estonian Ministry of Education and Science (grants SF0140077s08 and SF0140007s11). OK acknowledges as well RF President grant for young researchers MD-99.2010.5 and Federal Target Program "Research and scientific-pedagogical cadres of Innovative Russia" for 2009-2013, as part of the event 1.2.1 (Contracts 518 and 851).